Int J Clin Exp Pathol 2017;10(6):6665-6673
www.ijcep.com /ISSN:1936-2625/IJCEP0049659

Original Article

Differential expression of long non-coding RNAs in prostatic carcinoma cell line LNCaP after occurrence of androgen independent transformation

Wu Zhou[1], Zhongyong Wang[1], Zhihua Tao[2], Lili Ji[1], Beibei Zhou[1], Mo Shen[1], Hongxiang Tu[1]

[1]Department of Medical Laboratory, The First Affiliated Hospital of Wenzhou Medical University, Wenzhou, PR China; [2]Department of Medical Laboratory, School of Medicine, The Second Affiliated Hospital of Zhejiang University, Hangzhou, PR China

Received January 24, 2017; Accepted April 23, 2017; Epub June 1, 2017; Published June 15, 2017

Abstract: Prostate cancer (PCa) is a common malignant tumor of the urinary system in men. It has long aroused special attention because of its likelihood to undergo androgen independent transformation during the course of androgen-deprivation therapy. Recent studies suggested that long non-coding RNAs (lncRNAs) played crucial roles in human diseases including cancer. The aim of the study was to investigate the role of lncRNAs in the process of androgen independent transformation of PCa cells. We compared lncRNA expression profiles of PCa cell lines LNCaP cells and LNCaP androgen-independent cells (LNCaP-AI cells) after the occurrence of androgen independent transformation using Human LncRNA Array containing 30,586 lncRNAs and 26,109 mRNAs (Human LncRNA Array v3.0, Arraystar, Inc.). Using microarray data, we identified 2,766 differentially expressed lncRNAs and 1,895 differentially expressed mRNAs (≥3.0 fold-change, $P \leq 0.001$) between LNCaP and LNCaP-AI cells. Among them, 899 lncRNAs and 1151 mRNAs were up-regulated, while 1,867 lncRNAs and 744 mRNAs were down-regulated. Using qRT-PCR, a selection of differentially expressed lncRNA and coding mRNA transcripts including *AR*, *PSA, LncRNA NR_027708* and *ENST00000479270* was confirmed. Gene ontology (GO) bioinformatics analysis highlighted that many processes were highly expressed in the LNCaP-AI cells during the course of growth. Dysregulation of some of these lncRNAs may play important roles in cholesterol metabolism and nutrient uptake. In this study, we demonstrated that a large number of lncRNAs may play important roles in driving LNCaP cells to undergo androgen independent transformation. These transcripts are potential molecular targets for preventing LNCaP cells from transforming to LNCaP-AI cells.

Keywords: Prostate cancer, long non-coding RNA (lncRNA), mRNA, array, androgen independent transformation

Introduction

Prostate cancer (PCa) is the second most prevalent cancer in men worldwide [1]. Since the pioneering discovery of PCa response to castration or the administration of estrogens by Huggins and Hodges in 1941 [2], androgen ablation has been generally employed as a therapy for metastatic PCa patients for whom prostatectomy or radiotherapy is no longer indicated. However, despite the initial therapeutic efficacy of androgen ablation, androgen-dependent tumors may eventually become androgen-independent. Over a period of 18-20 months, tumor cells begin growing rapidly and PSA level increases again. The median survival of such patients is only 1-2 years [3]. The molecular mechanism underlying the switch from androgen-dependent to androgen-independent prostate tumors remains poorly understood. Long non-coding RNAs (lncRNAs) are defined as RNA transcripts larger than 200 nucleotides that do not appear to have protein-coding potential. Accumulating evidence indicates that lncRNAs are key regulators of diverse biological processes such as transcriptional regulation, cell growth and differentiation [4-8]. Aberrant expression of lncRNAs is known to be associated with various human cancers. In our previous study, we successfully cultivated androgen dependent LNCaP cells that could survive in the environment without androgen, and we named

them as LNCaP-AI cells [9]. The aim of the present study was to examine differences in expression profiles of lncRNA and mRNA between LNCaP-AI cells (treatment group) and LNCaP cells (control group) using third-generation lncRNA microarray, hoping that it could help gain insights into the role of lncRNAs in PCa switch from the androgen-dependent to androgen-independent form.

Materials and methods

Cell culture

Human PCa LNCaP cells (Cell Bank of the Chinese Academy of Sciences, Shanghai, China) were maintained in DMEM/F12 (Gibco, Grand Island, NY, USA) supplemented with 10% fetal bovine serum (FBS) (Gibco, Grand Island, NY, USA). By gradually reducing the androgen concentration in liquid culture, LNCaP cells were cultivated into LNCaP-AI cells [9] LNCaP-AI cells were maintained in DMEM/F12 (1:1) (Gibco, Grand Island, NY, USA) supplemented 10% FBS by activated carbon glucan treatment (Gibco, Grand Island, NY, USA). All cells were maintained at 37°C in a humidified incubator with 5% CO_2 and sub-cultured every 4-6 days.

RNA extraction and RNA quality control

Total RNA was extracted using Trizol reagent (Invitrogen, Carlsbad, CA, USA) and purified with an RNeasy Mini Kate (Qiagen Hilden, Germany) according to manufacturer's protocol. RNA quantity and quality were measured by NanoDrop ND-1000. RNA integrity was assessed by standard denaturing agarose gel electrophoresis.

Microarray

Arraystar Human LncRNA Microarray V3.0 is designed for the global profiling of human LncRNAs and protein-coding transcripts, about 30,586 LncRNAs and 26,109 coding transcripts can be detected by it.

RNA labeling and array hybridization

Sample labeling and array hybridization were performed according to the Agilent One-Color Microarray-Based Gene Expression Analysis protocol (Agilent Technology) with minor modifications. Briefly, mRNA was purified from total RNA after removal of rRNA (mRNA-ONLY™ Eukaryotic mRNA Isolation Kit, Epicentre). Then, each sample was amplified and transcribed into fluorescent cRNA along the entire length of the transcripts without 3' bias utilizing a random priming method (Arraystar Flash RNA Labeling Kit, Arraystar). The labeled cRNAs were purified by RNeasy Mini Kit (Qiagen). The concentration and specific activity of the labeled cRNAs (pmol Cy3/μg cRNA) were measured by NanoDrop ND-1000. Each labeled cRNA (1 μg) was fragmented by adding 5 μl 10× Blocking Agent and 1 μl 25× Fragmentation Buffer, then heated at 60°C for 30 min, and finally 25 μl 2× GE Hybridization buffer was added to dilute the labeled cRNA. Hybridization solution (50 μl) was dispensed into the gasket slide and assembled to the LncRNA expression microarray slide. The slides were incubated for 17 h at 65°C in an Agilent Hybridization Oven. The hybridized arrays were washed, fixed and scanned using the Agilent DNA Microarray Scanner (part number G2505C).

Data analysis

Agilent Feature Extraction Software (version 11.0.1.1) was used to analyze the acquired array images. Quantile normalization and subsequent data processing were performed by using the GeneSpring GX v12.1 Software Package (Agilent Technologies). After quantile normalization of the raw data, LncRNAs and mRNAs that had at least 2 out of 4 Present or Marginal flags in "All Targets Value" were chosen for further data analysis. Differentially expressed LncRNAs and mRNAs with statistical significance between the two groups were identified through *P*-value/FDR filtering. Differentially expressed LncRNAs and mRNAs between the two samples were identified through Fold Change filtering. Hierarchical Clustering and combined analysis were performed using homemade scripts. Pathway and GO analyses were applied to determine the roles that these differentially expressed mRNAs played in these biological pathways or GO terms.

Quantitative real-time PCR (qRT-PCR)

The expression pattern of selected lncRNAs and mRNAs in additional samples was confirmed by qRT-PCR. Reverse transcription reaction was performed using 2 μg total RNA and reverse transcribed into cDNA using Oligo

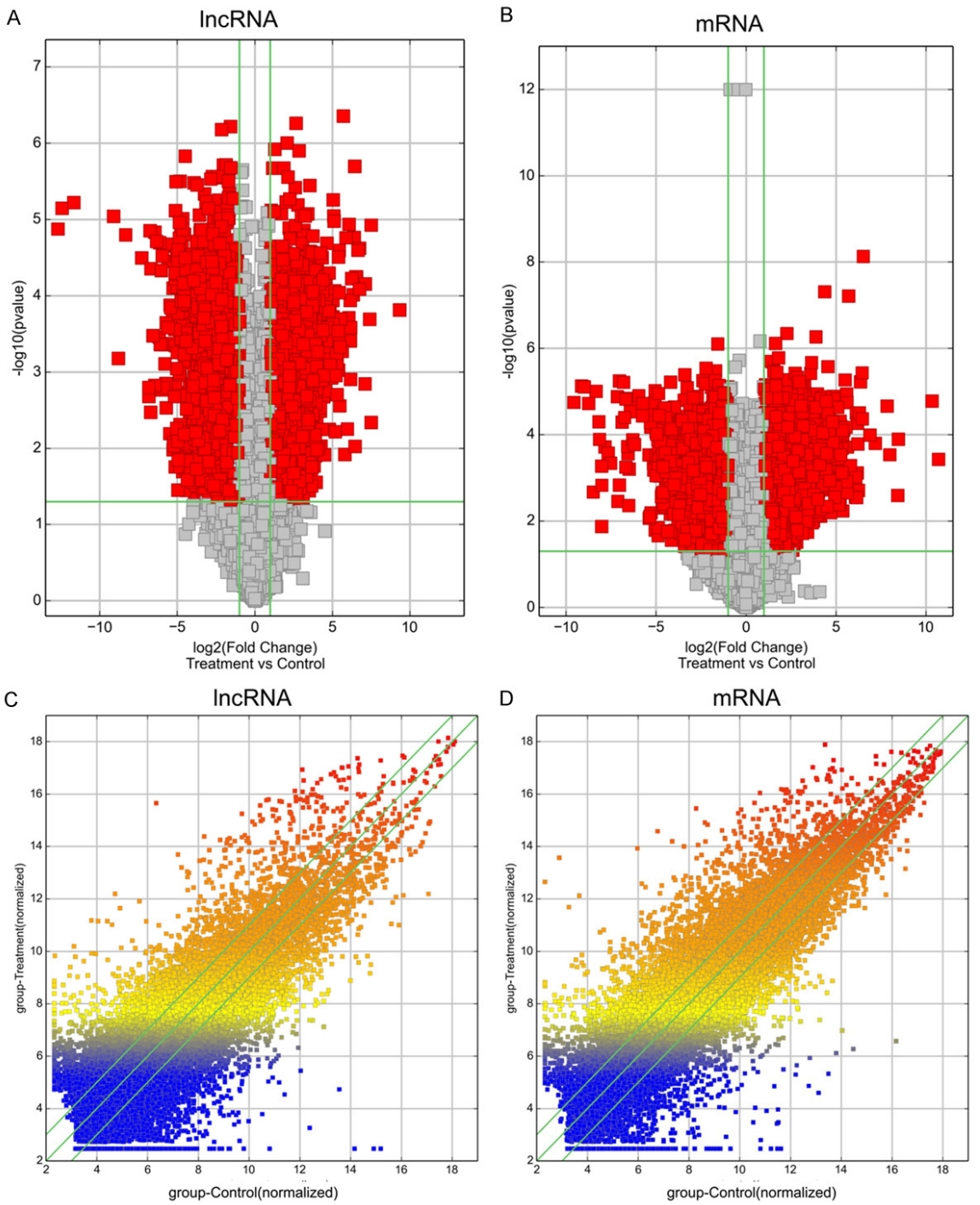

Figure 1. LncRNA and mRNA microarray expression data, volcano plots between *LNCaP cells (control group) and* LNCaP-AI cells *(treatment group)*. Microarray data were log-transformed and normalized using quantile normalization. After filtering to remove unreliable transcripts, the remaining was statistically analyzed to identify lncRNAs and mRNAs with significant differential expression. (A) lncRNA and (B) mRNA volcano plots of LNCaP-AI cells *versus LNCaP cells* (fold-change ≥3.0 and P≤0.001). Each square represents a different transcript. Transcripts are distributed according to statistical significance (y-axis) and the magnitude of change (log2 ratio LNCaP-AI cells: *LNCaP cells)* (x-axis). Red squares represent genes that pass the statistical and fold-change cut-offs. (C) lncRNAs above the top green line and below the bottom green line indicates a more than 3.0-fold change in lncRNAs between the two cell groups. (D) mRNAs above the top green line and below the bottom green line indicates a more than 3.0-fold change in mRNAs between the two cell groups.

(dT)18/Random Hexamers primer with RevertAid First Strand cDNA Synthesis Kit (Fermentas, Burlington, Canada) according to the manufacturer's instructions. The resulting cDNA was used as the template for qRT-PCR. Oligo nucleotide primers were synthesized (Life Technologies Corporation Invitrogen, Shanghai, China), and quantitative PCR reactions were performed in 20 μl containing 2 μl template cDNA, 10× SYBR Green master mix (Applied Biosystems, Life Technologies, USA), and 5 μmol of each primer. Amplification was performed using the ABI7500 PCR system (Applied Biosystems, Life Technologies, USA) with the expression of target genes relative to the reference genes *GAPDH* and *B2M*, determined using the 2(-ΔΔCt) method [10]. Amplification was repeated three times for each target gene, and the mean gene expression was calculated and used for statistical analysis. All qRT-PCR experiments included no-template controls. PCR products were examined by agarose gel electrophoresis using 2% (w/v) LE agarose (Seakem) stained with GoldView (Sbsbio, Beijing, China).

Results

LncRNA and mRNA expression profiles in LNCaP and LNCaP-AI cells

Microarray profiling of 30,586 lncRNAs (**Figure 1A**) and 26,109 coding transcripts (**Figure 1B**) was carried out using Arraystar Human LncRNA Microarray v3.0 (Kangcheng, Shanghai, China). The lncRNAs and coding transcripts collected from the most authoritative databases including RefSeq, UCSC Known Genes, Ensembl and the associated literature were detected by the microarray. The microarray work was performed by KangChen Bio-tech (Shanghai, China).

A total of 2,766 differentially expressed lncRNAs were identified between LNCaP and LNCaP-AI cells (fold change ≥3, P≤0.001) (**Figure 1C**). Among them, 899 were consistently up-regulated, and 1,867 lncRNAs were down-regulated. In total 1,895 mRNAs were differentially expressed using the fold-change threshold of 3.0, among which 1,151 were up-regulated, and 744 were down-regulated after progression from the androgen-dependent to androgen-independent form under an androgen-deprived environment of LNCaP-AI cells (**Figure 1D**).

GO analysis

Gene Ontology (GO) analysis was performed to determine the gene and gene product attributes in molecular functions, biological progresses and cellular components. It was found that numerous biological processes were involved, and the highest enriched GOs targeted by up-regulated transcripts were DNA strand elongation involved in DNA replication (GO: 0006271; ontology: Biological process; *P*= 1.0808E-12) (**Figure 2A**), condensed nuclear chromosome, centromere region (GO: 0000780; ontology: Cellular component; *P*=0.0009) (**Figure 2B**) and molecular function (GO: 0008409; ontology: 5'-3' exonuclease activity; *P*=0.0059) (**Figure 2C**). The highest enriched GOs targeted by down-regulated transcripts were positive regulators of Rho protein signal transduction (GO: 2000060; ontology: Biological process; *P*=0.0022) (**Figure 2D**), ER membrane protein complex (GO: 0072546; ontology: Cellular component; *P*=0.0416) (**Figure 2E**), and cis-trans isomerase activity (GO: 0016859; ontology: Molecular function; *P*= 0.0033) (**Figure 2F**).

Pathway analysis

Pathway analysis showed that 31 pathways corresponded to the up-regulated transcripts, and the most enriched network was "Cell cycle-Homo sapiens (human)" (Fisher-*P* value =2.35E-15) composed of 61 targeted genes (**Figure 3A**). At the same time, 24 pathways corresponded to the down-regulated transcripts, and the two most enriched networks were "Endocytosis-Homo sapiens (human)" (Fisher-*P* value =1.12E-3) composed of 45 targeted genes and "transcriptional misregulation in cancer-Homo sapiens (human)" (Fisher-*P* value =1.86E-3) composed of 40 targeted genes (**Figure 3B**). Among these pathways, the "prostate cancer" pathway showed that genes in the "*PI3K-ERK*" pathway were up-regulated in LNCaP-AI cells in the androgen-free environment, which enabled cells to proliferate and survive. The androgen receptor (*AR*)-prostate specific antigen (*PSA*) pathway was also up-regulated in LNCaP-AI cells (**Figure 3C**). These results are consistent with the previous report and the clinical finding that *PSA* is elevated when androgen independent transformation occurs in PCa patients [11, 12].

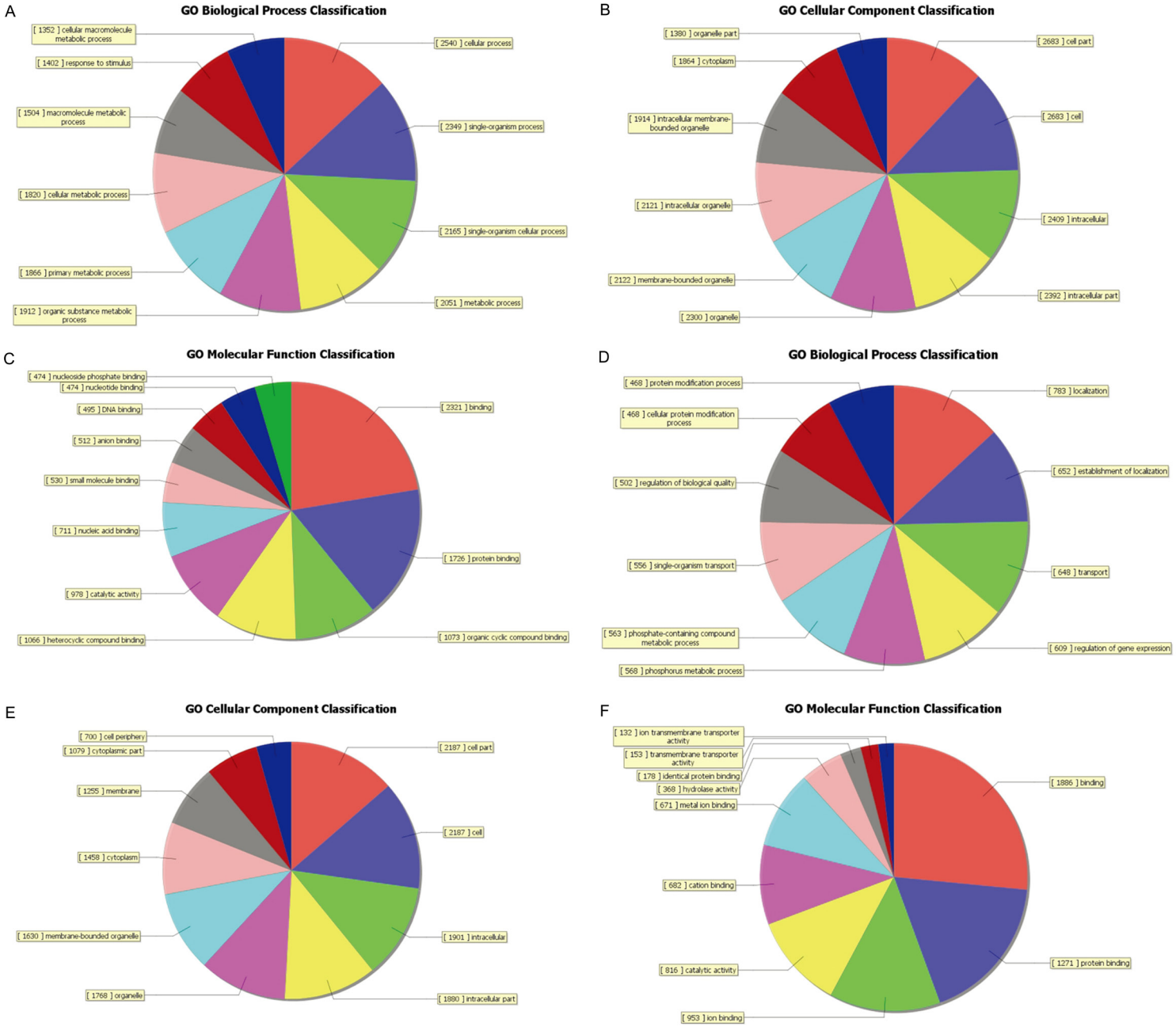
A
GO Biological Process Classification
[1352] cellular macromolecule metabolic process
[1402] response to stimulus
[1504] macromolecule metabolic process
[1820] cellular metabolic process
[1866] primary metabolic process
[1912] organic substance metabolic process
[2540] cellular process
[2349] single-organism process
[2165] single-organism cellular process
[2051] metabolic process
B
GO Cellular Component Classification
[1380] organelle part
[1864] cytoplasm
[1914] intracellular membrane-bounded organelle
[2121] intracellular organelle
[2122] membrane-bounded organelle
[2300] organelle
[2683] cell part
[2683] cell
[2409] intracellular
[2392] intracellular part
C
GO Molecular Function Classification
[474] nucleoside phosphate binding
[474] nucleotide binding
[495] DNA binding
[512] anion binding
[530] small molecule binding
[711] nucleic acid binding
[978] catalytic activity
[1066] heterocyclic compound binding
[2321] binding
[1726] protein binding
[1073] organic cyclic compound binding
D
GO Biological Process Classification
[468] protein modification process
[468] cellular protein modification process
[502] regulation of biological quality
[556] single-organism transport
[563] phosphate-containing compound metabolic process
[568] phosphorus metabolic process
[783] localization
[652] establishment of localization
[648] transport
[609] regulation of gene expression
E
GO Cellular Component Classification
[700] cell periphery
[1079] cytoplasmic part
[1255] membrane
[1458] cytoplasm
[1630] membrane-bounded organelle
[1768] organelle
[2187] cell part
[2187] cell
[1901] intracellular
[1880] intracellular part
F
GO Molecular Function Classification
[132] ion transmembrane transporter activity
[153] transmembrane transporter activity
[178] identical protein binding
[368] hydrolase activity
[671] metal ion binding
[682] cation binding
[816] catalytic activity
[953] ion binding
[1886] binding
[1271] protein binding

Figure 2. The Gene ontology project provides a controlled vocabulary to describe gene and gene product attributes in any organism (http://www.geneontogy.org). The ontology covers three domains: Biological Process (BP), Cellular Component (CC) and Molecular Function (MF). Fisher's exact test was used to see whether there was more overlap between the DE list and the GO annotation list than would be expected by chance. The *p*-value denotes the significance of GO terms enrichment in the DE genes. The lower the *p*-value, the more significant GO term (*P*-value ≤0.05 is recommended). A-C. The highest enriched GOs targeted by up-regulated transcripts. A. BP; B. CC; C. MF; D-F. The highest enriched GOs targeted by down-regulated transcripts. D. BP; E. CC; F. MF; A-F. The chart shows the top ten counts of the significant enrichment terms.

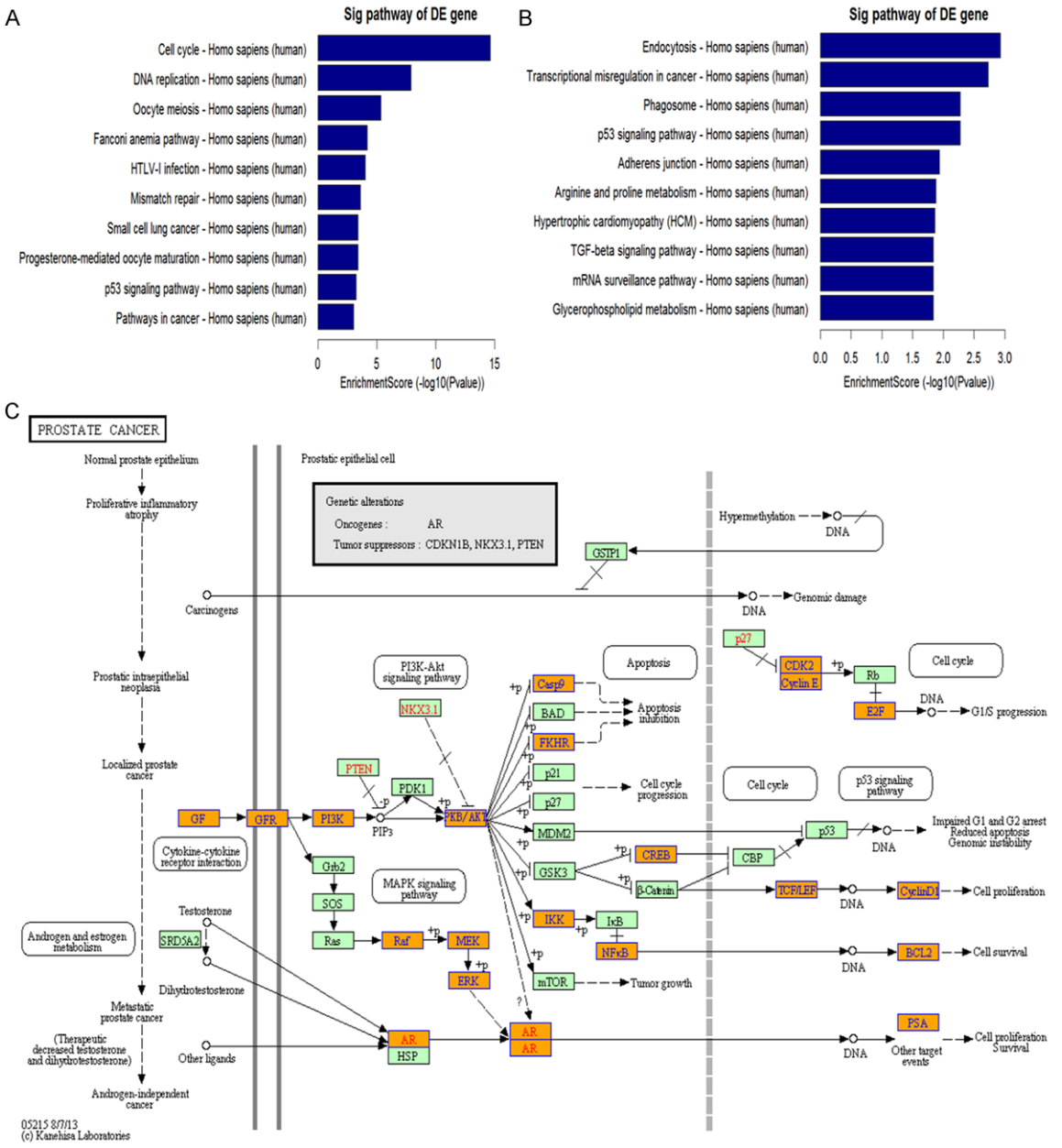

Figure 3. Pathway analysis is a functional analysis mapping genes to KEGG pathways. The *P*-value (EASE-score, Fisher-*P* value or Hypergeometric-*P* value) denotes the significance of the pathway correlated to the conditions. The lower the *p*-value, the more significant the pathway is. (The recommended *p*-value cut-off is 0.05.). A. Pathways correspond to the up-regulated transcripts. B. Pathways correspond to the down-regulated transcripts. A, B. The bar plot shows the top 10 enrichment score (-log10 (*P* value)) values of the significant enrichment pathway. C. The schematic diagram of the gene category "PCa". Orange marked nodes are associated with up-regulated or only whole dataset genes, and green nodes have no significance.

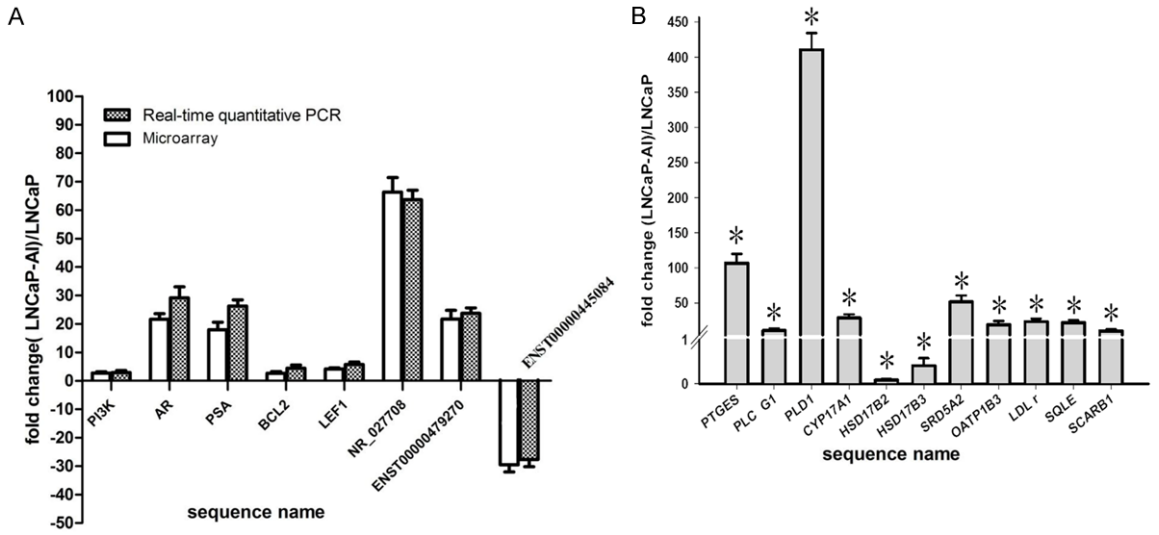

Figure 4. Comparison between microarray and qRT-PCR data for quantification of some genes. A. The Y-axis of the column in the chart represents the log-transformed median fold changes (Treatment/Control) in expression across seven samples ($P<0.05$). The qRT-PCR results are consistent with the microarray data. B. The black bars represent the relative expression levels of in LNCap-AI cells and LNCaP cells, *indicates a statistically significant difference ($P<0.05$) vs LNCaP cells in androgen and lipids metabolism. Each microarray and qRT-PCR data were normalized to internal controls (*GAPDH* and *ACTB*, two technical replicates each). Results are presented as log2-fold change ± SEM relative to the expression in LNCaP cells.

Validation of microarray data by qRT-PCR

To validate the microarray profiling expression data, the expression of *AR, PSA, BCL2, LEF1* and *LncRNA NR_027708* (associated withlipid metabolism), *ENST00000479270* (associated with macropinocytosis) and *ENST0000044-5084* were examined by qRT-PCR on additional LNCaP and LNCaP-AI cell samples (**Figure 4A**). Both microarray and qRT-PCR showed that the four genes and LncRNA were also up-regulated, confirming that the microarray data were reliable and stable.

As a number of abnormal mRNA expression of lipid metabolism enzymes could be observed in the microarray, we then compared the expression of some lipids metabolism and androgen synthase mRNA such as *PLD1, CYP17A1, SDR5A2,* et al. in LNCaP-AI cells by qRT-PCR (**Figure 4B**).

Discussion

Early genome research showed that only 1-2% human genomes were responsible for protein coding, and other non-coding regions were considered unless “junk DNAs”, especially those extensively transcribed “non-coding” RNAs, which were considered the “noise” of transcription. However, increased numbers of studies have demonstrated that these non-coding RNAs including LncRNAs possess biological functions [13, 14]. Recent evidence suggests that they may play major biological roles in cellular development and human diseases. Through regulating the gene expression of coding proteins or directly controlling transcription, LncRNAs can exert their carcinogenic or carcinostatic [15-17]. So the dysregulation of lncRNAs appears to be a significant feature of many complex human diseases, especially cancer, and LncRNAs may be a potential marker for the diagnosis or progression of cancer [18-20].

Our previous study found that when LNCaP-AI cells survived successfully in the androgen-free environment, the amount of mRNA expression of enmyzmes related to cholesterol transport and androgen metabolism would undergo changes [21]. In the present study, we used Arraystar Human LncRNA Microarray V3.0 to examine 30,586 LncRNAs and 26,109 coding transcripts in an attempt to see whether LncRNA participated in the process of anddrogen independent transformation. This is the first time to use microarray analysis to observe differential expression profiles of LncRNAs and

mRNAs after the occurrence of anddrogen independent transformation in LNCaP cell lines.

Using Arraystar Human LncRNA Microarray V3.0 data, we detected thousands of expressed lncRNAs in both LNCaP and LNCaP-AI cells. Other than changes in the amount of mRNA expression of enmyzmes related to cholesterol transport and androgen metabolism that we observed in our prior study, we also found that 899 LncRNAs and 1151 mRNAs were up-regulated, and that they were mostly involved in the cell cycle, endocytosis and transcriptional misregulation in LNCaP cancercells, though the function of most of these RNAs remains unknown.

Pathway analysis showed that genes associated with proliferation and anti-apoptosis were activated in LNCaP-AI cells, along with up-regulation of *PI3K-AKT* pathways. The phenomenon of *AR* and *PSA* elevation is consistent with the findings of other studies on androgen independent PCa. However, the reason why genes associated with proliferation and anti-apoptosis were activiated in LNCaP-AI cells in an androgen-free environment remains unanswered. In addition, upregulated mRNA level of enzymes in androgen and lipids metabolism indicated that the androgen-independent transformation of LNCaP cells might express androgen for cell survival using lipids in the androgen-free environment.

Several studies reported aberrant lncRNA expression in various types of human cancers in cluding PCa [22-24]. It was found in our study that when LNCaP cells transformed to LNCaP-AI cells in the process of androgen independent transformation, the expression level of *NR_027708* (assoicated with cholestoral metabloism), *ENST000004792709* (associated with macropinocytosis) and *ENST0000044-5084* lncRNAs was elevated significantly, indicating that these lncRNAs not only aprticipated in the occureence of PCa but played an important role in the process of androgen independent transformation. Therefore, a deeper understanding about LncRNAs may help identify more effective therapeutic targets and promote the development of new personalized therapeutic strategies.

In summary, this is the frist study to compare the expression profiles of LNCaP cells and LNCaP-AI cells. Deeper study about the abnormal change of these mRNA and lncRNAs may help reveal the mechanism of PCa cells undergoing androgen independent transformation, thus improving the efficacy of PCa diagnosis and treatment by finding effective therapeutic targets and developing new personalized therapeutic strategies.

Acknowledgements

This work was supported by grants from the National Natural Science Foundation of China (Grant No. 81202026); the Health and Family Planning Commission of Zhejiang Province (Grant No. 2015KYB243); and the “Youth Elite Project (Grant No. qnyc027)” of the First Affiliated Hospital of Wenzhou Medical University.

Disclosure of conflict of interest

None.

Address correspondence to: Wu Zhou, Department of Medical Laboratory, The First Affiliated Hospital of Wenzhou Medical University, Wenzhou 325000, Zhejiang, PR China. Tel: (86) 577-57779726; E-mail: gonewithwind95@163.com

References

[1] Jemal A, Siegel R, Xu J and Ward E. Cancer statistics, 2010. CA Cancer J Clin 2010; 60: 277-300.

[2] Huggins C and Hodges CV. Studies on prostatic cancer: I. The effect of castration, of estrogen and of androgen injection on serum phosphatases in metastatic carcinoma of the prostate. 1941. J Urol 2002; 168: 9-12.

[3] Heidenreich A, von Knobloch R and Hofmann R. Current status of cytotoxic chemotherapy in hormone refractory prostate cancer. Eur Urol 2001; 39: 121-130.

[4] Engreitz JM, Ollikainen N and Guttman M. Long non-coding RNAs: spatial amplifiers that control nuclear structure and gene expression. Nat Rev Mol Cell Biol 2016; 17: 756-770.

[5] Angrand PO, Vennin C, Le Bourhis X and Adriaenssens E. The role of long non-coding RNAs in genome formatting and expression. Front Genet 2015; 6: 165.

[6] Bao TP, Wu R, Cheng HP, Cui XW and Tian ZF. Differential expression of long non-coding RNAs in hyperoxia-induced bronchopulmonary dysplasia. Cell Biochem Funct 2016; 34: 299-309.

[7] Bouckenheimer J, Assou S, Riquier S, Hou C, Philippe N, Sansac C, Lavabre-Bertrand T,

Commes T, Lemaitre JM, Boureux A and De Vos J. Long non-coding RNAs in human early embryonic development and their potential in ART. Hum Reprod Update 2016; 23: 19-40.

[8] Dey BK, Mueller AC and Dutta A. Long non-coding RNAs as emerging regulators of differentiation, development, and disease. Transcription 2014; 5: e944014.

[9] Xu G, Mao YJ, Chen BH, He JJ, Tao ZH, Lin XM, Chen ZG, Shen M. [Establishment of an androgen-independent prostate cancer cell line induced by the combined of flutamide and androgen-free environment (Chinese)]. Chinese Journal of Cell Biology 2009; 31: 373-378.

[10] Livak KJ and Schmittgen TD. Analysis of relative gene expression data using real-time quantitative PCR and the 2(-Delta Delta C(T)) Method. Methods 2001; 25: 402-408.

[11] Keizman D, Huang P, Carducci MA and Eisenberger MA. Contemporary experience with ketoconazole in patients with metastatic castration-resistant prostate cancer: clinical factors associated with PSA response and disease progression. Prostate 2012; 72: 461-467.

[12] Dowling AJ, Panzarella T, Ernst DS, Neville AJ, Moore MJ and Tannock IF. A retrospective analysis of the relationship between changes in serum PSA, palliative response and survival following systemic treatment in a Canadian randomized trial for symptomatic hormone-refractory prostate cancer. Ann Oncol 2001; 12: 773-778.

[13] Carninci P and Hayashizaki Y. Noncoding RNA transcription beyond annotated genes. Curr Opin Genet Dev 2007; 17: 139-144.

[14] Kapranov P, Cheng J, Dike S, Nix DA, Duttagupta R, Willingham AT, Stadler PF, Hertel J, Hackermuller J, Hofacker IL, Bell I, Cheung E, Drenkow J, Dumais E, Patel S, Helt G, Ganesh M, Ghosh S, Piccolboni A, Sementchenko V, Tammana H and Gingeras TR. RNA maps reveal new RNA classes and a possible function for pervasive transcription. Science 2007; 316: 1484-1488.

[15] Han X, Wang L, Ning Y, Li S and Wang Z. Long non-coding RNA AFAP1-AS1 facilitates tumor growth and promotes metastasis in colorectal cancer. Biol Res 2016; 49: 36.

[16] Wang SS, Wuputra K, Liu CJ, Lin YC, Chen YT, Chai CY, Lin CS, Kuo KK, Tsai MH, Wang SW, Chen KK, Miyoshi H, Nakamura Y, Saito S, Hanafusa T, Wu DC, Lin CS and Yokoyama KK. Oncogenic function of the homeobox A13-long noncoding RNA HOTTIP-insulin growth factor-binding protein 3 axis in human gastric cancer. Oncotarget 2016; 7: 36049-36064.

[17] Ye N, Wang B, Quan ZF, Cao SJ, Wen XT, Huang Y, Huang XB, Wu R, Ma XP and Yan QG. Functional roles of long non-coding RNA in human breast cancer. Asian Pac J Cancer Prev 2014; 15: 5993-5997.

[18] Bussemakers MJ, van Bokhoven A, Verhaegh GW, Smit FP, Karthaus HF, Schalken JA, Debruyne FM, Ru N and Isaacs WB. DD3: a new prostate-specific gene, highly overexpressed in prostate cancer. Cancer Res 1999; 59: 5975-5979.

[19] Busch A, Eken SM and Maegdefessel L. Prospective and therapeutic screening value of non-coding RNA as biomarkers in cardiovascular disease. Ann Transl Med 2016; 4: 236.

[20] Zhou W, Tao Z, Wang Z, Hu W, Shen M, Zhou L, Wen Z, Yu Z, Wu X, Huang K, Hu Y and Lin X. Long noncoding RNA PCA3 gene promoter region is related to the risk of prostate cancer on Chinese males. Exp Mol Pathol 2014; 97: 550-553.

[21] Zhou W, Jiang Y, Ji L, Zhou L, Zhang M, Shen M, Zhao J, Tu H, Wang Z, Wu R, Chen Y, Zhou C, Huang K and Tao Z. Expression profiling of genes in androgen metabolism in androgen-independent prostate cancer cells under an androgen-deprived environment: mechanisms of castration resistance Int J Clin Exp Pathol 2016; 9: 8424-8431.

[22] Mouraviev V, Lee B, Patel V, Albala D, Johansen TE, Partin A, Ross A and Perera RJ. Clinical prospects of long noncoding RNAs as novel biomarkers and therapeutic targets in prostate cancer. Prostate Cancer Prostatic Dis 2016; 19: 14-20.

[23] Wang D, Ding L, Wang L, Zhao Y, Sun Z, Karnes RJ, Zhang J and Huang H. LncRNA MALAT1 enhances oncogenic activities of EZH2 in castration-resistant prostate cancer. Oncotarget 2015; 6: 41045-41055.

[24] Cui W, Qian Y, Zhou X, Lin Y, Jiang J, Chen J, Zhao Z and Shen B. Discovery and characterization of long intergenic non-coding RNAs (lincRNA) module biomarkers in prostate cancer: an integrative analysis of RNA-Seq data. BMC Genomics 2015; 16 Suppl 7: S3.